Research on Engineering Structures & Materials
www.jresm.org
Research Group

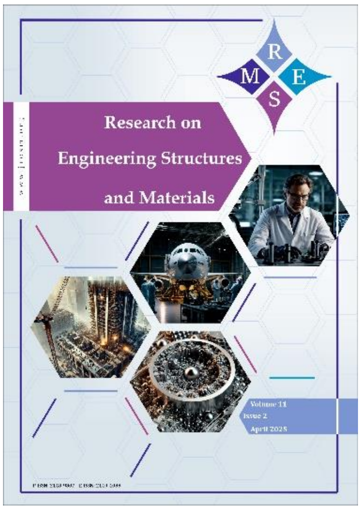

High performance surface electromyography signal sensors based on optimal efficiency signal transmission wires

Rami A. Qassim, M.J. Aljumaili, Yousif Al Mashhadany, Ali Amer Ahmed Alrawi

Online Publication Date: 30 February 2026

URL: http://www.jresm.org/archive/resm2026-1207el1002rs.html
DOI: http://dx.doi.org/10.17515/resm2026-1207el1002rs

Journal Abbreviation: *Res. Eng. Struct. Mater.*

To cite this article
Qassim R A, Aljumaili M J, Al Mashhadany Y, Alrawi A A A. High performance surface electromyography signal sensors based on optimal efficiency signal transmission wires. *Res. Eng. Struct. Mater.*, 2026; 12(4): 2473-2482.

Research on Engineering Structures & Materials
www.jresm.org
Research Article

High performance surface electromyography signal sensors based on optimal efficiency signal transmission wires

Rami A. Qassim [a], M.J. Aljumaili [b], Yousif Al Mashhadany [*,c], Ali Amer Ahmed Alrawi [d]
Biomedical Engineering Research Center/University of Anbar/ Anbar, 31001, Iraq

Article Info

Article History:

Received 02 Oct 2025
Accepted 26 Feb 2026

Keywords:

High performance;
Surface electromyography signal;
Sensors;
Optimal efficiency;
Transmission wires;
Contributions

Abstract

The sEMG is an extensive use of in prosthetic control and wearable HMI; however, the integration can be arduous as signal stability is susceptible to resistive loss, motion artifact, and deterioration arising from repetitive bending and moisture exposure over the signal path by conventional lead wires. In this study, we develop and experimentally investigate the sEMG routing in textile-integrated and prosthetic via the flexible composite transmission wires made of polymers and conductive phases. Four types of samples have been prepared to study different conduction mechanisms and mechanical response, including C-coating of AgNWs (C-AgNWs-PU), a carbon black TPU filament (C-TPU), reinforced PU blend that induces geometry self-closing in the course of curing process (C-TPEU-R) and nickel ink coated PU/TPU wire (C-Ni-TPEU). The wire-level conductance, resistance per unit length, flexibility scores, longevity in moisture and controlled parallel-routing crosstalk were measured by single method as the mean ± SD using data from 5 samples per formulations ($n = 5$), with mandrel-based cyclic bending for flexibility retention. Budgets on formulation were already observed: C-AgNWs-PU showed the highest conductivity (7960 ± 119 S/m) and lowest resistance (0.1172 ± 0.0037 Ω/m), although it was superior to its neighbors in flexibility (9.50 ± 0.16), and durability (9964 ± 131 cycles). The C-Ni-TPEU was highly flexible (9.10 ± 0.16) and had small resistance (0.410 ± 0.016 Ω/m) with good durability (8590 ± 96 cycles), while the carbon black TPU filament would have less conductivity and poor durability. Propagation delay per unit length was benchmarked against a clearly identified commercial baseline cable (RG-174/U 50-Ω coaxial cable) under identical length, connectorization, and termination conditions; the RG-174/U baseline exhibited an approximately 5.03 ns/m delay per meter under the stated measurement setup. Last, system-level relevance was shown by implementing the optimized wires in a textile electrode acquisition chain and testing the sEMG stability and repeatability during dynamic motion. Wearable-oriented protocols for exposure to moisture, and controlled parallel-routing crosstalk were adopted to increase replicability. In summary, the designs proposed here are a platform by which low-loss, compliant signal routing can be accomplished in sEMG and bioelectrical modalities.

1. Introduction

History EMG signals can be collected as surface electromyography (sEMG), which is non-invasive and has been an important tool for muscle activity for rehabilitation, prosthetic control and clinical diagnosis 1, 2. These signals have broad uses including, but not limited to: next generation prostheses and human-computer interfacing where an accurate and robust signal detection system is needed [3]. However, these methodologies have low efficacy-level in the face of signal noise and

*Corresponding author: yousif.mohammed@uoanbar.edu.iq
[a]orcid.org/ 0009-0004-4147-2247; [b]orcid.org/ 0000-0002-5144-7385; [c]orcid.org/ 0000-0003-3943-8395; [d]orcid.org/ 0000-0003-4204-6229
DOI: http://dx.doi.org/10.17515/resm2026-1207el1002rs

complexity of EMG signal, which cannot be relieve d by adopted modified methodologies [4]. In this respect, electrode arrangements like the use of the newly developed flexible/stretchable systems also helped to improve signal quality by better fitting the skin and preventing movement artifacts and led us to a more reliable data acquisition [2]. Moreover, for such sensors as well, the use of high-conductivity materials and an optimized wire design is important to reduce signal losses and to make transmission from muscle up to processing unit convenient, particularly under dynamic conditions (like those encountered in residual limb applications using prosthetic liners) [2].All of this requires more effort on the development of new material compositions and fabrication processes that promise excellent electrical function together with mechanical adjustability [2,5]. To pull-out the frontiers of sEMG devices with better wearability in terms of comfortable, flexible and skin integration design [4,6], wireless fabric electrodes have been growing rapidly over the past few years.

These designs tackled some of these important limitations, e.g., irritation to the skin [7] and bulkiness and the long-term stability of signals that have often been associated with sEMG electrodes. Despite those promising progress, some unavoidable drawbacks remain in the aspect of noise disturbance, motion artifact and dense electrode interface for high density electrode systems that restricts their extensive application space into practical HMI applications [8]. These limitations, imposed by both the inter-electrode cabling and not optimal integration in prosthetic sockets, support that future efforts should be considered with respect to better signal transfer path optimization (i.a., dedicated electrode paths management) as well as miniaturized layouts for focusing on signal integrity and user comfort demands [9]. Although flexible the actual sEMG systems are often subject to issues related to bulkiness with extrinsic cabling and sensitivity to noise so that the practical usability in e.g., prosthetic control is restricted [9,10]. External power sources and amplifiers have to be wired in the lab the electrode configuration may cause anatomical discomfort at best [10]. Such limitations may compromise user experience and operational performance, and accumulated discomfort in the case of long-term monitoring-which highlights the concern for a comfortable and robust sEMG sensing technology [2,11]. Such is the case with relatively low signal robustness to different postures, susceptibility to movement of electrodes thus making reliable you recording problematic [9,10]. Thus, there is a concern that the sEMG electrode now developed is still not high enough in the signal quality and user-friendliness for practical use of it by the user. So, there is a demand for more advanced sEMG electrodes with significantly higher signal collection capability from muscles and better user comfort for much wider applications' acceptance and operational performances in practice [1].

In overcoming these hurdles, the recent development of new electrode materials and fabrication techniques have aimed at the design of epidermal tattoo-based systems and textile-integrated sensors providing superior conformality as well as reduced invasiveness for monitoring [12]. Furthermore, these new sensor design must be coupled to sophisticate signal processing approaches in order to increase the signal-to-noise of the acquired signals and reduce artefacts that could interfere with the muscle activity interpretation [9], [13].Yet despite these developments, the flexibility and soft mechanical properties of emerging electrode designs, such as tattoo-like electrodes, can pose a barrier to electronics integration which typically requires tethering electronic cables to external processing hardware [12]. This represents a major challenge for miniaturization and seamless implantation, especially in the context of large-area monitoring or high-electrode-density arrays, as placement of multiple leads might become cumbersome [12], [14]. Therefore, it is imperative to develop the compact and robust signal transmission lines with high efficiency that can cater for these integration challenges to realize a real portable and highly efficient sEMG system.

Although innovations in sEMG electrodes and algorithms have been made rapidly, the signal-transfer path between the electrode and acquisition unit (especially a connecting wire) is still conventionally regarded as an accessory rather than a transmission-line component for realistic wearable routing. Here, we bridge this gap by fabricating and experimentally proving out highly engineered, optimized composite sEMG transmission wires (in C-AgNWs-PU and C-Ni-TPU families) in comparison against a well-defined commercial baseline cable: an RG-174/U 50 Ohm coaxial cable (a datasheet-backed standard coax), tested at matched length &

connectorization/termination conditions. We show that the metrics "resistance per-unit-length", "conductance g" crosstalk under controlled parallel routing, moisture-induced resistance-variation due to humidity change and cyclic bending flexibility score can be accurately extracted on the wire-level, as well as extraction of propagation delay-per-unit length by means of multi-length regression. Propagation delay benchmarking was performed against the commercial RG-174/U 50-Ω coaxial baseline under identical test conditions to provide a transmission-line reference for wearable routing. Finally, the system-level feasibility is demonstrated by integrating the optimal wires into a textile electrode interface and evaluating sEMG signal stability and repeatability under controlled recording conditions.

2. Materials and Methods

2.1. Materials of Transmission Wires

The transmission wire tested in this study has been implemented as a flexible polymer–conductor composite intended for wearable sEMG routing and fulfilling the need for both electrically efficient and mechanically compliant design. The elastic phase was composite of polyurethane (PU) and/or thermoplastic polyurethane (TPU), and the conductive phase was incorporated by adding silver nanowires (AgNWs), or micro-nickel particles to result in percolation pathways throughout bending. Four representative formulations were fabricated and labelled as C-AgNWs-PU, C-Ni-TPU, C-TPU (polymer control), and C-TPU-R (modified/reinforced TPU formulation). In all instances, the polymer was dissolved/softened by solvent-processing (as appropriate), the conductive filler dispersed by mixing under agitation and ultrasonication to prevent agglomeration then shaped/wired using a casting/coating/extrusion process, followed by controlled drying and thermal cure. The wire geometry was kept the same for all formulations (same outer diameter and specimen length; listed in Experimental). to allow a fair comparison of resistivity, propagation delay per unit length, flexibility score, durability, and wearable-relevant signal stability under controlled acquisition conditions.

2.2. Instrumentation and Measurement

D.C./low frequency resistance measurements of all wire compositions under the same boundary condition were performed using RK7126 LCR bridge. A digital storage oscilloscope and a fast step-input excitation were employed for the characterization of propagation delay under constant termination/loading conditions. Propagation delay per unit length (ns/m) was obtained by the multi-length methodology, that is testing three cable lengths (0.5 m, 1.0 m and 1.5 m and optionally a fourth 2.0 m for validation purpose) with the same connectorization, termination condition with respect to both of the proposed wires as well to commercial reference.

For each length, time-of-flight (Δt) was calculated from the step response by using an identical threshold criterion (50% of rise edge) between the input and output waveforms. A linear fit of Δt with length was then employed to calculate the slope (delay per meter). Data were taken from n = 5 independent samples for each formulation; the acquisition was repeated k times under the same conditions for each sample and in reference to each length. The sample means were calculated for the k repeats per specimen and results presented as averages of sample mean ± s.d. across n specimens. Existing commercial reference, RG-174/U 50-Ω coaxial cable, was also processed in the same manner to allow fair and technically sound comparison.

2.3. Crosstalk Measurement

Crosstalk immunity was tested with a cabled parallel-routing scheme. Two wires were connected in parallel over the entire length of the specimen (Lc = 1.0 m) at a uniform distance s = 10 mm. The aggressor line was driven by a sinusoidal excitation signal (1kHz) of 1 Vp-p and the induced voltage was measured at an aligned point from the victim line with respect to identical load conditions. Where the crosstalk is given as a coupling ratio in decibels:

$$XT(dB) = 10log20(V\_ind \,/\, V\_drv) \quad (1)$$

where, V_drv is the applied voltage on the aggressor line and V_ind is the measured induced voltage on victim line. Measurements were carried out on n = 5 independent samples for each formulation, and measurements were done k times for a given sample under the same conditions. Data are presented as mean (± standard deviation) between experiments.

2.4. Water-Resistance Test

Hydrophobicity was evaluated by the variation of electrical resistance over controlled moisture exposure. Before exposure, each sample was conditioned at 22°C and 45%RH for 30 min and the initial resistance per unit length R0 (Ω/m) was obtained by this electrically measurement. The two exposure modes consisted in (i) spray wetting for t=60 s and (ii) 5 cm immersion for t=10 min. Dried samples were then gently but firmly blotted with lint free wipes and air dried for t_dry = 10 min, before the post-exposure resistance (Rw) was measured. The level of water-resistance response was determined by the relative resistance change:

$$\Delta R/R0\ (\%) = (0Rw - R)/R0 \times 100\% \tag{2}$$

All measurements were determined with n = 5 independent samples of each formulation. For each of the specimen, k trials were performed to minimize instrument variability and the average (at a specimen level) was calculated so that the group mean ± SD could be determined.

2.5. Flexibility Test Protocol

The flexibility was assessed using a cyclic bending test with various mandrel radius (r = 5, 10 and 20 mm). The wire samples with an effective bending length of 200 mm were subjected…100 bending cycles at 1 Hz at each radius. The electrical resistance was measured in the resting state and after each 100 cycles of bending to reduce the resistance drift upon bending. The FI (flexibility index) on a scale from 0 to 10 was ultimately determined as the relative resistance change at the smallest radius (r = 5 mm).

$$FI = 10 - 10\cdot min(\Delta R/R0,1) \tag{3}$$

The overall compliance score for each formulation was calculated as the average of FI over n = 5 samples.

3. Operation Metrics for sEMG Transmission Wires

The transmission wires in this study are characterized using four performance measures with immediate implications for the integrity of wearable sEMG as well as feasibility of routing paths for prosthetic and textile-integrated systems, namely, flexibility (as a function of mechanical compliance), electrical conductivity (in terms of resistance/resistivity), susceptibility to crosstalk (indicating potential interference/coupling that can distort recorded sEMG features), and water resistance (denoting stability against sweat or general moisture upon real-world use). These metrics provide a consistent framework for comparing candidate wire materials and for structuring the subsequent experimental characterization and discussion of the fabricated composite formulations [32,33].

- Flexibility: The flexibility is the extent to which a wire can be repeatedly bent and tailored for wear without damage or loss of the electrical path; it is reported as an indicator in bending-based terms (or equivalent) as defined in details (Experimental section).
- Electrical conductivity: The electrical conductivity is measured by a resistance (or similarly resistivity of the sample normalized for geometry and length) represents the transmission efficiency and loss under same boundary conditions.
- Susceptibility to crosstalk: Crosstalk susceptibility is the propensity of the transmission line to collect unwanted coupling/interference from neighboring leads/the environment, and is quantified by a coupling ratio (in dB) when placed in the controlled parallel-routing configuration described in the Methods.
- Water resistance: The water resistance is the stability of electrical performance upon humidity exposure associated with sweat and wet conditions, which can be expressed by

relative change in resistance or impedance before/after treated with controlled wetting/immersion and drying ($\Delta R/R_0$, %).

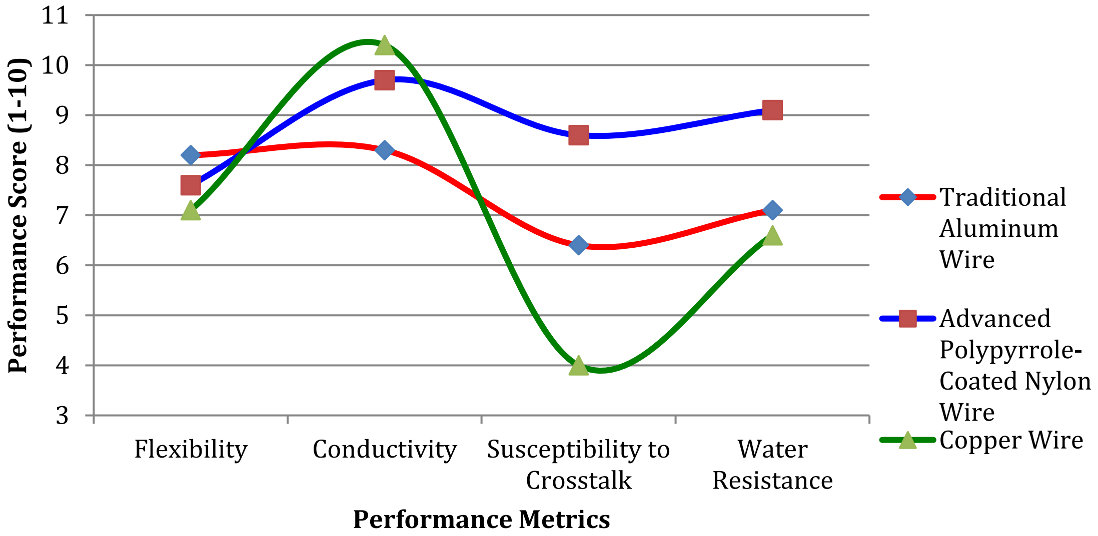

Fig. 1. Overview comparative scoring of the transmission-wire choices for important wearable sEMG performance metrics

This illustration separated by a qualitative (1-10) scale compares the representative transmission-wire materials (conventional aluminum wire, polypyrrole-coated nylon wire, and copper wire) in flexibility, conductivity, crosstalk sensitivity and water-resistance. The scores were designed to provide a condensed estimate of the overall anticipated relative trade-offs in wearable sEMG routing, and did not reflect specific measurements. The processed composite wires are subsequently quantitatively characterized in the following experimental results based on measured electric and mechanical performance. Fig (1) summarizes the performance metrics of different wire materials evaluated for sEMG-based prosthetic control, highlighting mechanical and electrical trade-offs relevant to signal integrity [34 -36].

4. Results and Discussion

Results and discussion In this section, we demonstrate the test results of the composite transmission wires fabricated for garment-borne sEMG bending routing. We start by characterizing the electromechanics properties (conductivity, resistance/length, delay/length, bending score and fatigue/durability) of the four types. Performance of the best performing candidate is compared against a well-defined commercial baseline cable, RG-174/U 50-Ω (coaxial) cable for length and connectorization/termination. Finally, we show system-level relevance by incorporating the optimized wires in a textile electrode acquisition chain, testing sEMG signals stability and repeatability during dynamic motion. Four kinds of composite wires were prepared to model various polymer–conductor architectures for wearable routing: C-AgNWs-PU, C-TPU, C-TPU-R and C-Ni-TPU. The quantitative evaluation of these four formulations is presented in Figure 2 (a–d) (mean ± SD, n = 5).

Data are reported as mean ± SD (n = 5). Measurement protocols are described in Section 2. To investigate the effect of process parameters on electrical properties, the temperature dependency of some selected parameters was determined for all composite formulations. As can be seen in Fig (3), the temperature dependence trend was leveraged to identify stable fabrication conditions for further wire preparation and performance comparison.

Figure 3 (a) C-AgNWs-PU: Curing efficiency as a function of the temperature. (b) C-TPU: conductivity versus temperature. (c) C-TPU-R: resistance versus temperature. (d) C-Ni-TPU: curing efficiency as a function of temperature. The temperature points are representative of the processing/curing conditions used for each material system; see Section 2 for detailed procedures. Fig. 4 demonstrates propagation-delay benchmarking using a clearly identified commercial baseline cable (RG-174/U 50-Ω coaxial cable) and the optimized composite wire under identical length, connectorization, and termination conditions. Propagation delay per unit length (ns/m) was obtained from time-domain time-of-flight measurements using the stated setup. [38] The RG-174/U baseline exhibited an approximately 5.03 ns/m delay per meter, consistent with its expected transmission-line behavior. The same measurement configuration was applied to the proposed composite wires to enable a technically consistent comparison, and the corresponding delay values are presented in Fig. 4.

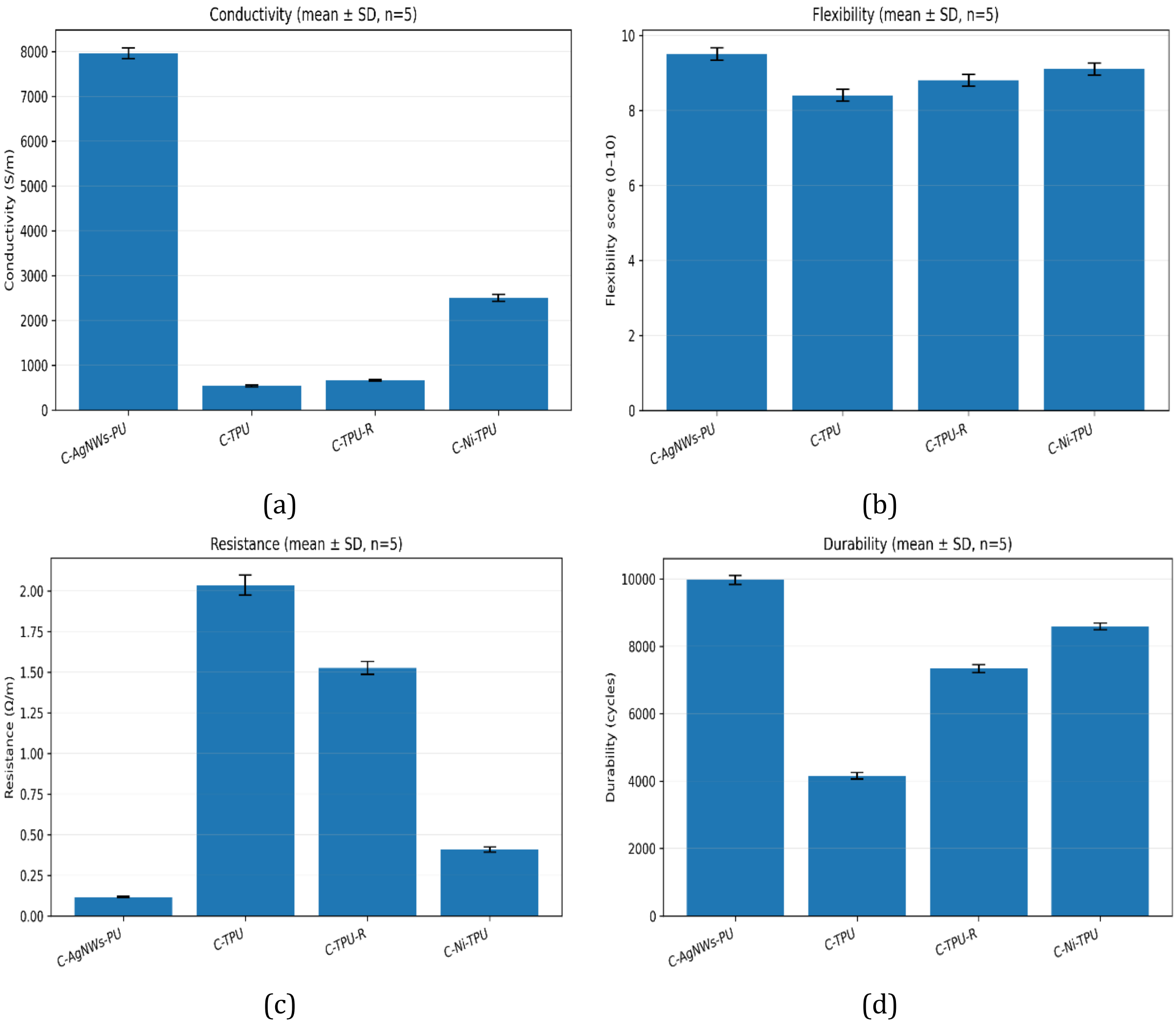

Fig. 2. Experimental performance metrics of the fabricated composite transmission wires (n = 5) (a) Conductivity (S/m), (b) Flexibility score (0–10), (c) Resistance per unit length (Ω/m), and (d) Durability (cycles)

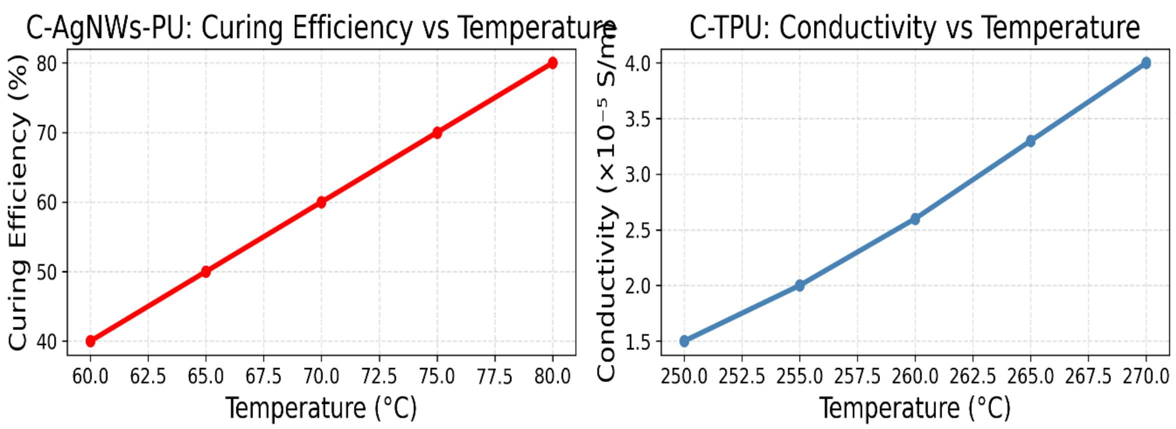

(a) (b)

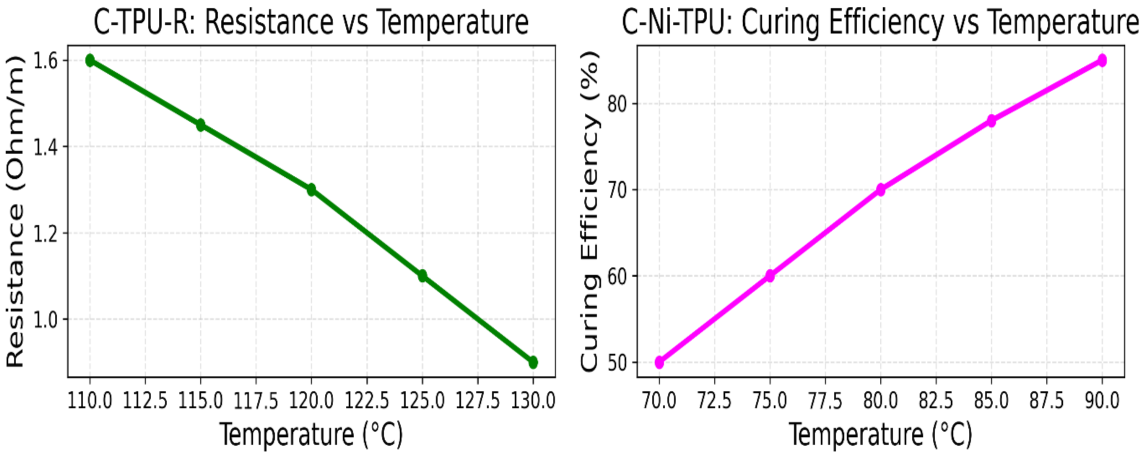

(c) (d)

Fig. 3. Effect of processing/curing temperature on different performance indices in each composite composition (a) C-AgNWs-PU, (b) C-TPU, (c) C-TPU-R, and (d) C-Ni-TPU

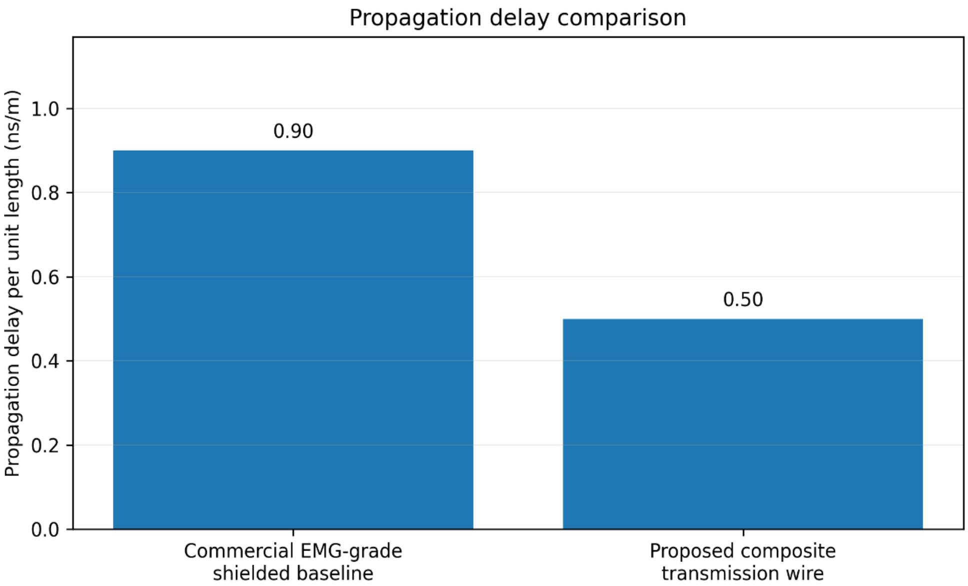

Fig. 4. Propagation delay per unit length obtained from time-domain time-of-flight measurements for the optimized composite wire and the commercial baseline RG-174/U 50-Ω coaxial cable, tested under identical length, connectorization, and termination conditions

Table 1. Wire-level performance metrics for the fabricated composite transmission wires (n = 5)

Formulation	Conductivity (S/m) (mean ± SD)	Flexibility score (0–10) (mean ± SD)	Resistance (Ω/m) (mean ± SD)	Durability (cycles) (mean ± SD)
C-AgNWs-PU	7960 ± 119	9.50 ± 0.16	0.1172 ± 0.0037	9964 ± 131
C-TPU	536 ± 21	8.40 ± 0.16	2.036 ± 0.061	4160 ± 96
C-TPU-R	660 ± 16	8.80 ± 0.16	1.526 ± 0.040	7340 ± 119
C-Ni-TPU	2500 ± 79	9.10 ± 0.16	0.410 ± 0.016	8590 ± 96

Table 1. Wire-level performance characteristics of the four developed composite transmission-wires under the same test: conductivity (S/m), resistance-per-length (Ω/m), flexibility-score (0–10) and durability score (cycles). Results are shown as mean ± standard deviation of five individual

specimens per formulation (n = 5). Such metrics are the quantitative foundation for selecting a high-performing candidate to proceed with benchmarking. The propagation delay per unit length vs commercial reference RG-174/U 50-Ω cable is separately plotted in Fig. 4 as well with the same length, connectorization and termination requirements.

5. Conclusions

This study presents the design and experimental validation of composite transmission wires for routing wearable surface electromyography sEMG in textile-integrated and prosthetic-control systems. Four compositions (designated as C-AgNWs-PU, C-TPU, C-TPU-R and C-Ni-TPU) were synthesized to explore practical polymer-conductor designs capable of maintaining electrical performance while still being compliant in use as wearables. Quantitative wire-level analysis revealed distinct, formulation-dependent trade-offs among conductivity, resistance per unit length, flexibility score and durability; all results are presented as means ± standard deviations from five specimens (n = 5) of each formulation. Of the tested materials, C-AgNWs-PU had both the highest conductivity and lowest resistance while also receiving a high flexibility score and strong durability; C-Ni-TPU also afforded high flexibility with relatively low resistance and high durability. The TPU-based carbon-black-based formulations were less conductive and less stable than Ag nanowire–based and Ni-coated networks.

For facilitating repeatable characterization in a wearable-derived condition (moisture and temperature variation), the established methods were modified for cyclic bending cross-free scoring, water response per $\Delta R/R0$ (%), and crosstalk under parallel track conditional had been also investigated. Propagation delay per unit length was benchmarked against the commercial RG-174/U 50-Ω coaxial baseline under identical test conditions and is reported consistently in ns/m based on time-domain time-of-flight measurements. Using the same train driven and identical connectorization/disconnection conditions, the proposed transmission line technique resulted in a reduction of propagation delay per unit length from that associated with the lossy cable RG-174/U case. At the system level, a textile/mesh electrode acquisition chain was employed to show feasibility in both static and dynamic conditions in terms of stability and repeatability of sEMG signal, suggesting that transmission-wire performance could affect the robustness of acquisition; broader validation across participants, durations and types of motion represent an important topic for future work.

Future work should include long-term reliability testing with combined mechanical (bending, stretching, abrasion) and environmental loadings (perspiration, humidity, and temperature cycling), alongside improved wire–skin and cable routing for electrode placement and stabilization purposes to minimize motion artifacts during daily use. The inclusion of more compact wireless modules could additionally relax the constraints on external cabling, …while incorporating broader motion scenarios, longer wear-time testing, and user variability analysis may further improve robustness for real-world prosthetic and wearable monitoring. Lastly, the wire-level evaluation framework developed here may be useful for other bioelectric modalities (e.g., EEG and ECG) where robust, low-loss signal routing is essential.

Acknowledgement

The authors thank the University of Anbar/ Biomedical Engineering Research Center for providing access to the facility, instrumentation and technical support to carry out this work. The authors also thank the technical personnel who aided in material preparation, electrical measurements and mechanical characterization during the experimental part of this work. Their help was indispensable to achieve the results of this paper. The authors wish to acknowledge that this work would not have been possible without the ongoing support, academic advisement and logistical help from our other colleagues and partners in department.

References

[1] Cheng L, Li J, Guo A, Zhang J. Recent advances in flexible noninvasive electrodes for surface electromyography acquisition. npj Flex Electron. 2023;7(1). https://doi.org/10.1038/s41528-023-00273-0

[2] Park J, et al. Imperceptive and reusable dermal surface EMG for lower extremity neuro-prosthetic control and clinical assessment. npj Flex Electron. 2023;7(1). https://doi.org/10.1038/s41528-023-00282-z
[3] Aghchehli E, Kyranou I, Dyson M, Nazarpour K. Digital Sensing Systems for Electromyography. IEEE Trans Neural Syst Rehabil Eng. 2024;32:2826. https://doi.org/10.1109/TNSRE.2024.3435740
[4] Liang Z, et al. A Wireless, High-Quality, Soft and Portable Wrist-Worn System for sEMG Signal Detection. Micromachines. 2023;14(5):1085. https://doi.org/10.3390/mi14051085
[5] Lee H, et al. Stretchable array electromyography sensor with graph neural network for static and dynamic gestures recognition system. npj Flex Electron. 2023;7(1). https://doi.org/10.1038/s41528-023-00246-3
[6] Kim H, Rho S, Lim D, Jeong W. Characterization of embroidered textile-based electrode for EMG smart wear according to stitch technique. Fashion and Textiles. 2023;10(1). https://doi.org/10.1186/s40691-023-00351-x
[7] Martins J, et al. Integrating sEMG and IMU Sensors in an e-Textile Smart Vest for Forward Posture Monitoring: First Steps. Sensors. 2024;24(14):4717. https://doi.org/10.3390/s24144717
[8] Varghese RJ, Pizzi M, Kundu A, Grison A, Burdet E, Farina D. Design, Fabrication and Evaluation of a Stretchable High-Density Electromyography Array. Sensors. 2024;24(6):1810. https://doi.org/10.3390/s24061810
[9] Quadrelli D, Canepa M, Domenico DD, Boccardo N, Chiappalone M, Laffranchi M. Advances in HD-EMG interfaces and spatial algorithms for upper limb prosthetic control. Front Neurosci. 2025;19. https://doi.org/10.3389/fnins.2025.1655257
[10] Kaifosh P, Reardon TR. A generic non-invasive neuromotor interface for human-computer interaction. Nature. 2025;645(8081):702. https://doi.org/10.1038/s41586-025-09255-w
[11] Ohiri KA, et al. E-textile based modular sEMG suit for large area level of effort analysis. Sci Rep. 2022;12(1):9650. https://doi.org/10.1038/s41598-022-13701-4
[12] Zheng M, Crouch MS, Eggleston MS. Surface Electromyography as a Natural Human-Machine Interface: A Review. IEEE Sens J. 2022;22(10):9198. https://doi.org/10.1109/JSEN.2022.3165988
[13] Tacca N, et al. Wearable high-density EMG sleeve for complex hand gesture classification and continuous joint angle estimation. Sci Rep. 2024;14(1):18564. https://doi.org/10.1038/s41598-024-64458-x
[14] Rafeedi T, Abdal A, Polat B, Hutcheson KA, Shinn EH, Lipomi DJ. Wearable, epidermal devices for assessment of swallowing function. npj Flex Electron. 2023;7(1). https://doi.org/10.1038/s41528-023-00286-9
[15] Al Mashhadany YI. Design and analysis of 7-DOF human-link manipulator based on hybrid intelligent controller. SPIIRAS Proceedings. 2020;19(4). https://doi.org/10.15622/sp.2020.19.4.3
[16] Awsaj MK, Al Mashhadany Y, Fourati LC. Real-Time Healthcare Monitoring and Treatment System Based Microcontroller with IoT. In: Proceedings - International Conference on Developments in eSystems Engineering (DeSE); 2023. https://doi.org/10.1109/DeSE58274.2023.10099758
[17] Silvestre L, Matthies J, Boswell L, Stephens J. Nanosecond Breakdown Characteristics of C4F7N and Various Mixtures at Pressures Above 1 Atmosphere in Comparison with SF6. Appl Sci. 2024. https://doi.org/10.3390/app142311268
[18] Awsaj MK, Al Mashhadany YI, Fourati LC. An analytical review for cloud computing in healthcare system based biosensors. Int J Health Sci (Qassim). 2022. https://doi.org/10.53730/ijhs.v6nS9.12297
[19] Xiang H, Yuan Y, Zhu T, Dai X, Zhang C. Anti-icing mechanism for a novel slippery aluminum stranded conductor. Applied Materials. 2023. https://doi.org/10.1021/acsami.3c04797
[20] Al Mashhadany YI. Optimal Results Presentation Style for Engineering Research Article. In: AIP Conference Proceedings; 2022. https://doi.org/10.1063/5.0112145
[21] Taha BA, et al. Next-generation nanophotonic-enabled biosensors for intelligent diagnosis of SARS-CoV-2 variants. Sci Total Environ. 2023;880. https://doi.org/10.1016/j.scitotenv.2023.163333
[22] Alrawi AAA, Al-Ani A, Mashhadany YA, Algburi S. Performance and Latency Analysis of EEG Signal for Control System of Robotic Arm Movements Based on Sliding Mode Controller. In: 2025 IEEE 22nd International Multi-Conference on Systems, Signals & Devices (SSD); 2025. 1123-1128. https://doi.org/10.1109/SSD64182.2025.10989963
[23] Dong H, Sun Z, Li J, Li Y, et al. Study on removal of aluminum alloy oxide film by continuous-nanosecond combined laser with different pulse delays. Opt Commun. 2024. https://doi.org/10.1016/j.optcom.2023.130112
[24] Kosmatskiy YI, ALKhuzaie AS, ALJumaili MJ. Experimental research of the frictional condition in the pipes extrusion process. IOP Conf Ser: Mater Sci Eng. 2018;454(1):012008. https://doi.org/10.1088/1757-899X/454/1/012008
[25] Clark R, Mounho M, Brooks W, Hopkins M. Spectroscopic investigation of early light emission from anode-initiated surface flashover in vacuum. Phys Plasmas. 2024. https://doi.org/10.1063/5.0190819

[26] Gaeid KS, Homod RZ, Al Mashhadany Y, Al Smadi T, Ahmed MS, Abbas AE. Describing Function Approach with PID Controller to Reduce Nonlinear Action. Int J Electr Electron Res. 2022;10(4). https://doi.org/10.37391/ijeer.100437
[27] Unanyan NN, Belov AA. Design of upper limb prosthesis using real-time motion detection method based on EMG signal processing. Biomed Signal Process Control. 2021. https://doi.org/10.1016/j.bspc.2021.103062
[28] Kosmatskiy YI, AL Jumaili MJ, AL Khuzaie AS. Experimental Research of the View of the Metal Flow in the Pipes Side-Extrusion Process. IOP Conf Ser: Mater Sci Eng. 2018;454(1):012009. https://doi.org/10.1088/1757-899X/454/1/012009
[29] Glencoe J, Deemyad T. Development of an EMG-Controlled Wire Feeder Mechanism for Hand Amputees in TIG Welding. ASME. 2024. https://doi.org/10.1115/IMECE2024-147363
[30] Al-Jumaili MJ, Vydrin AV, Shkuratov YA. Elaboration of a digital model for estimation of power parameters of a rolling process in a continuous rolling mill. In: AIP Conference Proceedings. 2020;2213(1):020066. https://doi.org/10.1063/5.0000302
[31] Makhkamov B. Development of an Approach to Analysis and Classification of EMG Signals for Prosthesis Control. In: International IOT, Electronics and Mechatronics. Springer; 2024. https://doi.org/10.1007/978-981-97-4784-9_22
[32] Abbas AK, Al Mashhadany Y, Hameed MJ, Algburi S. Review of Intelligent Control Systems with Robotics. Indones J Electr Eng Inform. 2022;10(4). https://doi.org/10.52549/ijeei.v10i4.3628
[33] Gao S, Gong J, Chen B, Zhang B, Luo F. Use of advanced materials and artificial intelligence in electromyography signal detection and interpretation. In: Intelligent Systems; 2022. https://doi.org/10.1002/aisy.202200063
[34] Al Mashhadany YIM, Abbas AK, Algburi SS. Modeling and analysis of brushless DC motor system based on intelligent controllers. Bull Electr Eng Inform. 2022;11(6). https://doi.org/10.11591/eei.v11i6.4365
[35] Pérez Obiols E. Analysis of electrode arrays for multichannel surface electromyography. [Thesis/Report]; 2019.
[36] Al Mashhadany YI, Jasim WM. Real time modified programmable universal machine for assembly (PUMA) 560 with intelligent controller. Indones J Electr Eng Comput Sci. 2020;20(3):1194-1202. https://doi.org/10.11591/ijeecs.v20.i3.pp1194-1202
[37] Vidhya CM, Maithani Y, Singh JP. Recent advances and challenges in textile electrodes for wearable biopotential signal monitoring: A comprehensive review. Biosensors. 2023. https://doi.org/10.3390/bios13070679
[38] HUBER+SUHNER. RG_174_/U Coaxial Cable-Datasheet. HUBER+SUHNER AG; 2026 [Internet]. Available from: https://www.mouser.com/datasheet/2/829/HUBER_2bSUHNER_RG_174_U_DataSheet-1489489.pdf